International Journal of Nanomedicine

Dovepress
open access to scientific and medical research

Open Access Full Text Article

ORIGINAL RESEARCH

Ultra-Small Lysozyme-Protected Gold Nanoclusters as Nanomedicines Inducing Osteogenic Differentiation

This article was published in the following Dove Press journal:
International Journal of Nanomedicine

Kuo Li[1,*]
Pengfei Zhuang[1,2,*]
Bailong Tao[3]
Dan Li[1,2]
Xuejiao Xing[1]
Xifan Mei[1]

[1]Department of Orthopedics, School of Pharmaceutical Science, The First Affiliated Hospital of Jinzhou Medical University, Jinzhou, People's Republic of China; [2]Department of Basic Science, School of Pharmaceutical Science, Jinzhou Medical University, Jinzhou, People's Republic of China; [3]Key Laboratory of Biorheological Science and Technology, Ministry of Education College of Bioengineering, Chongqing University, Chongqing 400044, People's Republic of China

*These authors contributed equally to this work

Purpose: Ultra-small gold nanoclusters (AuNCs), as emerging fluorescent nanomaterials with excellent biocompatibility, have been widely investigated for in vivo biomedical applications. However, their effects in guiding osteogenic differentiation have not been investigated, which are important for osteoporosis therapy and bone regeneration. Herein, for the first time, lysozyme-protected AuNCs (Lys-AuNCs) are used to stimulate osteogenic differentiation, which have the potential for the treatment of bone disease.

Methods: Proliferation of MC3T3E-1 is important for osteogenic differentiation. First, the proliferation rate of MC3T3E-1 was studied by Cell Counting Kit-8 (CCK8) assays. Signaling pathways of PI3K/Akt play central roles in controlling proliferation throughout the body. The expression of PI3K/Akt was investigated in the presence of lysozyme, and lysozyme-protected AuNCs (Lys-AuNCs) by Western blot (WB) and intracellular cell imaging to evacuate the osteogenic differentiation mechanisms. Moreover, the formation of osteoclasts (OC) plays a negative role in the differentiation of osteoblasts. Nuclear factor κB ligand (RANKL) and macrophage colony-stimulating factor (M-CSF) signaling pathways are used to understand the negative influence of the osteogenic differentiation by the investigation of Raw 264.7 cell line. Raw 264.7 (murine macrophage-like) cells and NIH/3T3 (mouse fibroblast) cells were treated with tyloxapol, and the cell viability was assessed. Raw 264.7 cells have also been used for in vitro studies, on understanding the osteoclast formation and function. The induced osteoclasts were identified by TRAP confocal fluorescence imaging. These key factors in osteoclast formation, such as (NFATc-1, c-Fos, V-ATPase-2 and CTSK), were investigated by Western blot.

Results: Based on the above investigation, Lys-AuNCs were found to promote osteogenic differentiation and decrease osteoclast activity. It is noteworthy that the lysozyme (protected template), AuNPs, or the mixture of Lysozyme and AuNPs have negligible effects on osteoblastic differentiation compared to Lys-AuNCs.

Conclusion: This study opens up a novel avenue to develop a new gold nanomaterial for promoting osteogenic differentiation. The possibility of using AuNCs as nanomedicines for the treatment of osteoporosis can be expected.

Keywords: nanoclusters, bone, osteogenic differentiation, osteoporosis

Introduction

Osteoporosis is a disease that can cause bone loss silently, leading to a great susceptibility to fragile fractures for humans.[1,2] Nowadays, the clinical treatment of osteoporosis mainly depends on traditional drugs, such as bisphosphonates, androgens, the combination of vitamin D and calcium supplements.[3–5] However,

Correspondence: Xifan Mei
Tel +86 13504064506
Email meixifan@jzmu.edu.cn

submit your manuscript | www.dovepress.com
DovePress
http://doi.org/10.2147/IJN.S241163

osteoporosis is still not completely curable using these treatments, which fail to offer long-term solutions.[6–8] For instance, significant side effects occur due to their drug-resistant problems.[9–11]

Recently, the application of biocompatible nanomedicines shows the potential for the safe treatment of osteoporosis.[12,13] For instance, the gold nanoparticles (AuNPs) have been reported to be effective for osteoporosis treatment without causing toxic effects.[14] They are efficient for the promotion of osteoblast differentiation,[15,16] suppression of the formation of osteoclast,[17] and inhibition of adipose-derived stem cell differentiation.[15,18] Especially, low drug-resistant problems have generated using AuNPs-related nanomedicines.[19] However, most of these AuNPs (5–100 nm) related medicines are still difficult to be cleaned from the body because of their large sizes.[20] The remaining gold is still a concern for safe medication. It is of great importance to further improve these gold related nanomedicines for the therapy of osteoporosis to decrease this concern.

Metal Nanoclusters (NCs), smaller than 3 nm,[21] have been extensively studied in biomedical applications, such as bioimaging, drug delivery, photo-thermal treatment, etc.[22,23] In our previous work, ultra-small copper nanoclusters (CuNCs) were found to be promising for the osteoporosis therapy based on the in vitro study.[24] However, it is well known that copper is quite unstable. The release of copper ions may also cause toxic problems.[25] Compared to CuNCs, AuNCs are much more stable and little ions can be released in bioculture.[26] The AuNCs have shown higher safety and efficiency for therapy of in vivo diseases, such as the cancers,[27] bacterial infections[28] and Parkinsons,[29] compared to other nanomedicines including CuNCs and larger AuNPs. They can be cleaned from the body efficiently because of their ultra-small sizes.[30] Herein, we found Lys-AuNCs were effective for both promoting osteogenic differentiation and inhibiting osteoclast formation. This indicates Lys-AuNCs have great potential for rebuilding the bone and will be promising for the treatment of bone diseases such as Osteoporosis. To the best of our knowledge, this is the first investigation that uses AuNCs for potential therapy of Osteoporosis.

Materials and Methods

Instrument

The inductively coupled plasma mass spectrometry (ICP-MS) (Thermo Scientific) was used to determine the concentration of NCs. Ultraviolet–visible spectroscopy (UV-vis) absorption spectra of the samples were recorded by UV-1600 Spectrophotometer (Beijing Rayleigh Analytical Instrument). Transmission electron microscopy (TEM) images were carried out on a JEOL 2010 microscope operating at 200 kV. The fluorescent cell imaging was studied with a microscope (Olympus, Tokyo, Japan). Fluorescence intensities were read by a microreader (Varioskan Flash, Thermo Scientific, Waltham, MA, USA). The autoradiograms were carried out on an Alpha Innotech Photodocumentation System (Alpha Innotech Corporation). The relative absorbance of the bands, which represent the amount of protein expression, was analyzed using Quantity One software (The Discovery Series).

Materials and Reagents

Mouse osteoblastic cells (MC3T3-E1), Mouse fibroblast cell line (NIH-3T3) and the popular murine macrophage cell lines (Raw 264.7) were obtained from the American Type Culture Collection (ATCC). The Gibco Dulbecco's Modified Eagle Medium: Nutrient Mixture F-12 (DMEM/F-12), 10% Fetal Bovine Serum (FBS), 1% Penicillin-Streptomycin (PS), the phosphate-buffered saline (PBS), 4-(1, 1, 3, 3-Tetramethylbutyl) cyclohexyl-polyethylene glycol (Triton X-100), the Tris(hydroxymethyl) aminomethane (Tris–HCl), the sodium dodecyl sulfate-polyacrylamide gel (SDS-PAGE) , Alexa Fluor 546-labeled anti-rabbit IgG and the Alexa Fluor 488-labeled anti-mouse IgG were purchased from Thermo Fisher Scientific Incorporation. The Recombinant Human Macrophage Colony-stimulating Factors (M-CSF) were purchased from R&D Systems Incorporation. The Recombinant Murine sRANK Ligands (RANKL) were purchased from PeproTech Incorporation. The Radio Immunoprecipitation assay lysis buffers (RIPA), the Phenylmethanesulfonyl fluorides (PMSF), the ALP Staining Kits, ALP Activity Assay Kits and 3-(4,5-Dimethylthiazol-2-yl)-2,5-diphenyltetrazolium bromide (MTT) cell proliferation and cytotoxicity assay kits were purchased from Beyotime Company. The Polyvinylidene Fluorides (PVDF) was purchased from Merck Millipore Limited. The Chemiluminescence kits were purchased from Pierce Chemical Company. The Alpha Innotech Photo documentation System was purchased from Alpha Innotech Corporation. The Cell Counting Kit-8 (CCK-8) was purchased from Dojindo Lab. The Collagen-1 (Col-1) antibodies, Glyceraldehyde-3-phosphate dehydrogenase (GAPDH) antibodies, the Cellular oncogene fos (c-Fos) antibodies and Nuclear factor of activated T-cells-1 (NFATc-1) antibodies were purchased from Cell Signaling Technology Incorporation. The 4% Paraformaldehyde (PFA)

and the Alizarin Red Staining were purchased from Solarbio Company Limited. The alkaline phosphatase antibodies (ALP), β-Tubulin antibodies, Phospho-phosphatidylinositol 3-kinase (p-PI3K) antibodies, Phosphatidylinositol 3-kinase (PI3K) antibodies, Phospho-Auto-ja Kuljetusalan Työntekijäliitto (p-Akt) antibodies, Auto- ja Kuljetusalan Työntekijäliitto antibodies (Akt), the Tartrate-Resistant Acid Phosphatase (TRAP) and the Filamentous actin antibodies (F-actin) were purchased from Affinity LLC. The Vacuolar-type-H+-ATPase antibodies (V-ATPase-d2) and Cathepsin K antibodies (CTSK) were purchased from Santa Cruz biotechnology Incorporation.

Cell Culture

MC3T3-E1 cells were cultured in a DMEM-F12 medium containing 10% FBS. The cultures were maintained at 37°C in a fully humidified atmosphere of 5% CO_2 in the air. The culture mediums were changed every 3 days. NIH-3T3 cells were cultured in a DMEM medium containing 10% FBS. The cultures were maintained at 37°C in a fully humidified atmosphere of 5% CO_2 in the air. The culture mediums were changed every 3 days. In osteoblast proliferation experiments, the cells were divided randomly into 3 groups: (1) Control groups: the cell cultures were used without any further treatment; (2) Lysozyme groups: 50 μM lysozyme was added to the cell culture mediums; (3) AuNPs groups: 50 μM AuNPs were added to the cell culture mediums; (4) Lysozyme- AuNPs groups: 50 μM lysozyme- AuNPs were added to the cell culture mediums; (5) Lysozyme-AuNCs groups: 50 μM lysozyme-AuNCs were added to the cell culture mediums.

The Raw 264.7 cells were stimulated with DMEM mediums containing 10%FBS, 25 ng/mL of M-CSF, and 50 ng/mL of RANKL for 5 days. The cell cultures were maintained at 37°C in a fully humidified atmosphere of 5% CO_2 in the air and the culture mediums were changed every 3 days.

Cell Viability

The cell viability of Raw 264.7 and NIH-3T3 was studied based on cell count MTT assay analysis. First, the cells were seeded in 96-well plates at a density of 4×10^3 per well and incubated overnight. In addition, the two types of cells were exposed to the mediums for 24 hours in the absence (control) and in the presence of 5, 10, 20, 40, 80, 160, 320 μM Lys-AuNCs, respectively. Next, the culture solution was discarded and carefully washed with PBS for 2–3 times. Then 20 μL of MTT solution (5mg/mL) was added to each well and the plate was incubated at 37 ° C and 5% CO_2 for 4 hours until a purple-colored formazan product was developed. After the media were carefully removed, the purple products were dissolved in 150 μL of dimethyl sulfoxide (DMSO). The absorbance was recorded at 450 nm by a microplate reader to investigate the cell viability.

Proliferation of MC3T3-E1 Cells

The proliferation of MC3T3-E1 was investigated based on Cell Counting Kit-8 (CCK8) assays. First, the cells were seeded at a density of 4×10^3 per well in a 96-well plate and incubated overnight. Furthermore, the cells were exposed to the mediums in the absence (Control), and the presence of 50 μM of lysozyme, and 50 μM of Lys-AuNCs for 1 day respectively. Next, the cells were treated the same way for 4 and 7 days. The plates were incubated at 37 °C with 5% CO_2 for 4 hours until a purple-colored formazan product was developed. The absorbance was recorded at 450 nm by a microplate reader.

Confocal Fluorescence Imaging

In each group, MC3T3-E1 cells were washed 3 times by PBS after incubating for a certain time. Then, these cells were fixed by 4% PFA for 30 min. Subsequently, the cells were washed by PBS 3 times and then blocked by 5% goat serum for 2 hours. After that, these cells were incubated in a culture medium with primary anti-ALP antibodies, Col-1 antibodies, p-PI3K antibodies, p-Akt antibodies, and anti-β-Tubulin antibodies for staying overnight at 4°C. Then, the cells were rinsed with PBS 3 times. Subsequently, these cells were incubated with secondary antibodies (Alexa Fluor 546-labeled anti-rabbit IgG) and the anti-mouse IgG (Alexa Fluor 488-labeled anti-mouse IgG) (Invitrogen, Waltham, MA) for 2 hours and washed 3 times by PBS. Finally, the cells were stained by DAPI for 15 minutes. In the same way, the Raw 264.7 cells were cultured for 5 days. After washing, the mediums were incubated in a culture medium with the primary anti-TRAP antibodies, NFATc-1 antibodies, F-actin antibodies at 4°C overnight. Next, these cells were incubated with the corresponding secondary antibodies for 2 hours. Then, the cell imaging experiments were observed by single-photon confocal fluorescence microscopy.

Alizarin Red Staining Assay

The Alizarin red staining of MC3T3E-1 cells was used to evaluate the mineralization ability of Lys-AuNCs. The control group was treated in normal cell culture mediums

without adding any additional agent. The MC3T3-E1 was adhered to 6-well plates for 24 hours at 37 ° C with 5% CO_2 (cell count, ca. 4×10^5). On the 21st day, the cells without the addition of Lysozyme were used as a control. The cells were treated with 50 μM of lysozyme and 50 μM of Lys-AuNCs in DMEM/F-12. The mediums were fixed in 4% PFA for 10 minutes and stained with 0.1% alizarin red for 1 hour. Meanwhile, the cells were seeded in a 96-well plate using the same method. The absorbance was recorded at 562 nm using a microplate reader.

ALP Staining and Activity Assay

For ALP staining, MC3T3E-1 cells were seeded into 6-well plates and treated with 50 μM of Lysozyme and 50 μM of Lys-AuNCs respectively. The cells that have been treated with Lys-AuNCs for 7 days were fixed with 4% PFA for 15 minutes. Then, the cells were washed three times with PBS buffers and stained with an ALP Staining Kit. The MC3T3E-1 cells that have been treated with Lyzome-AuNCs for 7 days were lysed with a buffer (20 mM of Tris–HCl (pH 7.5), 1% Triton X-100, and 150 mM NaCl). After incubating at 37 °C for 30 minutes, the ALP activity was evaluated by measuring the absorbances at 405 nm using a Microreader.

Western Blot Analysis

To determine the protein expression of certain biomarkers related to osteogenesis, the protein extracts from the MC3T3E-1 cells (the 3 days after the induction of osteogenesis) and the Raw 264.7 cells that have been induced for 5 days were prepared in a RIPA buffer supplemented with a PMSF. The total proteins were separated by a 10% SDS-PAGE gel electrophoresis and then transferred to PVDF membranes. The membranes were then blocked in a 5% BSA medium at room temperature for 1 hour and then incubated overnight at 4 °C with antibodies specific to GAPDH, ALP, Col-1, p-PI3K, PI3K, p-Akt, Akt, TRAP, NFATc-1, c-Fos, V-ATPase-d2, and CTSK respectively. Subsequently, they were treated with a corresponding secondary antibody for 2 hours. Immunoreactive proteins were revealed using an enhanced chemiluminescence kit. The expression of GAPDH was used as the control. The autoradiograms were carried out on an Alpha Innotech Photo documentation System. The relative absorbance of the bands, which represent the amount of protein expression, was analyzed using Quantity One software.

Synthesis of Lys-AuNCs

2.5 mL of Lysozyme solution (15 mg/L) was combined with 2.5 mL of aqueous $HAuCl_4$ (5 mM) solution in a 10 mL vial. Then, 100 μL of NaOH (100 mM) solution was introduced. The mixture was stirred well until transparent. Then, the vial was transferred to a 37 °C water bath and kept for 24 hours.

Synthesis of AuNPs

The AuNPs were synthesized according to a previously reported paper.[31] In a typical process, 100 mL of $HAuCl_4$ (0.25 mM) was put into a 250 mL flask at room temperature. After the solution was brought to boil while vigorously stirring, 0.7 mL of 5% sodium citrate solution was combined. The reaction was allowed to run until a wine-red color was obtained.

Statistical Analysis

All values are expressed as mean ± SD. The statistical analysis was performed using a SPSS 13.0 software (SPSS Inc., Chicago, IL, USA). Multiple comparisons were analyzed using a one-way analysis of variance followed by the Student-Newman-Keul tests.

Results and Discussion

Promotion of Osteogenic Activity

First, the formation of ultra-small AuNCs was confirmed by TEM (Figure S1). Cytotoxicity plays an important role to decide whether nanomedicine can be used for the therapy of disease. Herein, two different cell lines (NIH-3T3 and Raw 264.7) were employed to test the cell viability by the MTT method. The cells were studied in the presence of Lys-AuNCs from 0 to 320 μM. Interestingly, a dose-response pattern was not apparently seen in both cell lines when the concentrations are smaller than 320 μM. The cell viability of the cells is almost 100%. This indicates Lys-AuNCs show insignificant toxicity at this concentration range. Based on our previous study, 50 μM of Lys-AuNCs can promote MC3T3E1 (and important cells for the regeneration of the bone tissue) with the highest efficiency, which will be used for further investigations.[32] To evaluate the proliferation rate of MC3T3E1 grown at different time, the cell viability was measured following incubation of the MC3T3E1 cells in the absence and presence of Lysozyme and Lys-AuNCs at 50 μM. Figure 1 shows the effect of Lysozyme and Lys-AuNCs on the proliferation of MC3T3E-1 based on Cell Counting Kit 8

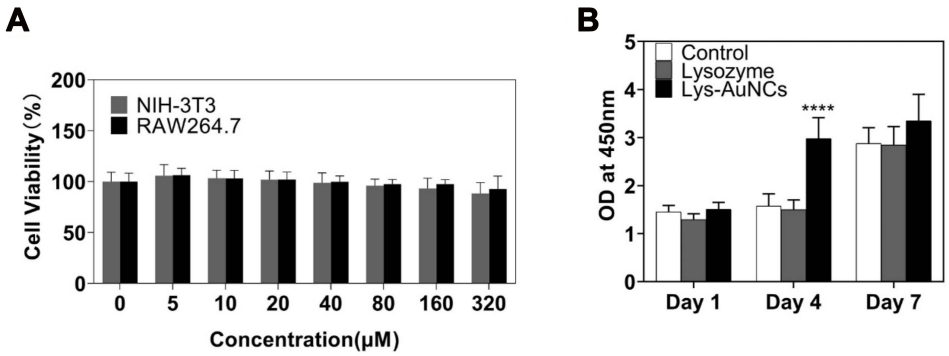

Figure 1 The toxicity of Lys-AuNCs on Raw 264.7 cells, NIH-3T3 cells, and MC3T3-E1 cells. (**A**) Cell viability of Raw 264.7 cells and NIH-3T3 cells treated with various concentrations of Lys-AuNCs (0, 5, 10, 20, 40, 80, 160, 320 μM) based on MTT Kits. (**B**) CCK-8 activity of MC3T3-E1 cells after 1 day, 4 days and 7 days for the Control and using Lysozyme and Lys-AuNCs as medicines. The statistically significant difference is presented as (****) $p < 0.001$ as compared to Lys-AuNCs.

(CCK-8) analysis. No significant difference for the cell viability of MC3T3E-1 was observed after 1 day compared to the control group after adding lysozyme and Lys-AuNCs. However, Lys-AuNCs obviously promoted the proliferation of MC3T3-1 after four days when the number of cells reached a high limit. Meanwhile, the lysozyme itself showed insignificant effects on increasing cell viability. This indicates the promotion of the proliferation rate is mainly attributed to the presence of AuNCs rather than the template (lysozyme). After that, the cells gradually proliferated respectively and the cell viabilities were comparable after 7 days for all the three groups including the Control, the lysozyme, and Lys-AuNCs. It can be concluded that Lys-AuNCs are not only showing low

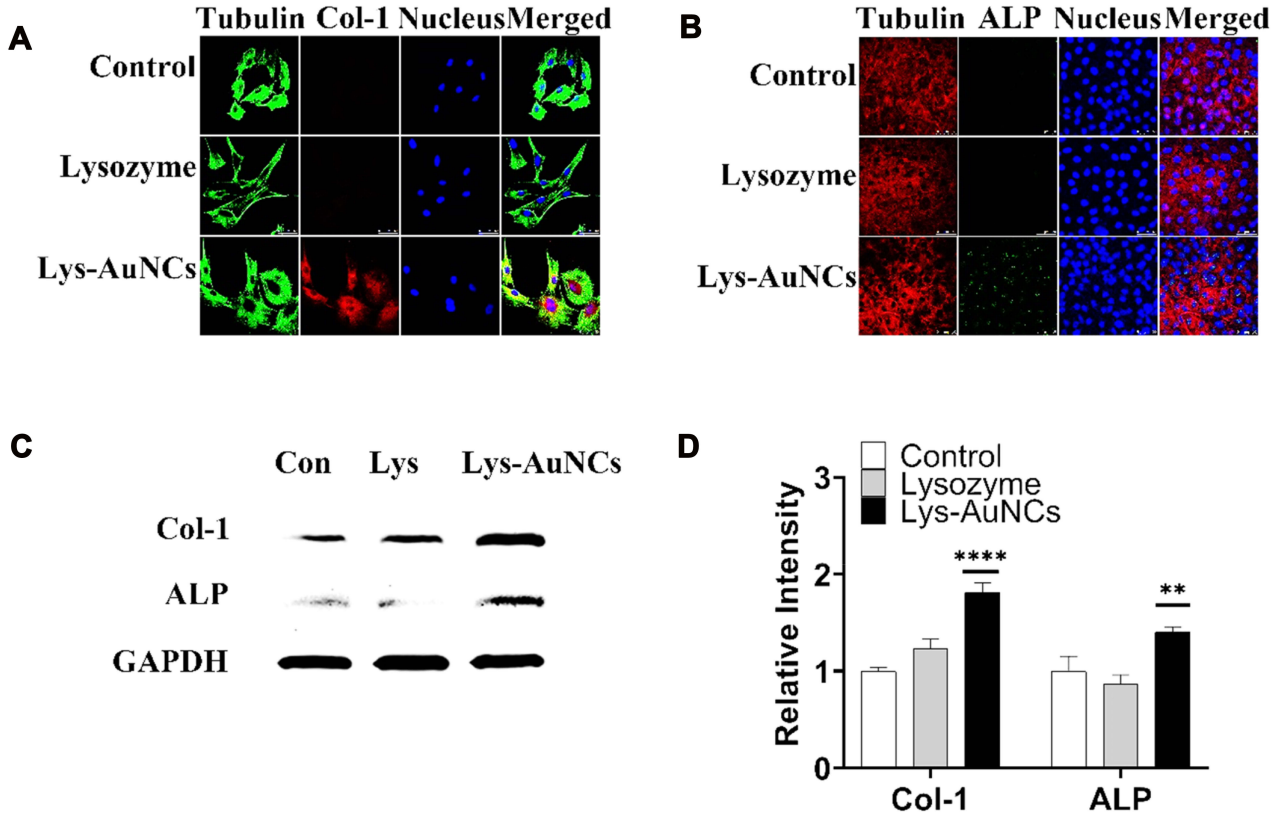

Figure 2 Effects of Lys-AuNCs on osteo-specific protein of MC3T3E-1. The confocal fluorescence imaging analyses showed that Lys-AuNCs increased the protein expression of Col-1 after 3 days (**A**) and ALP after 7 days (**B**). (**C**) WB analyses of osteo-specific proteins including Col-1 and ALP of osteogenesis on 3 days. (**D**) Relative quantitative analysis of WB analyses for Col-1 and ALP. Scale bar = 200 μm. **P < 0.01, ****P < 0.001 vs control group.

toxicity to mammalian cells but also enable the cells to proliferate much faster. Meanwhile, Lysozyme insignificantly influences the cell proliferation rate of MC3T3E1 compared to the control group.

Along with the cell proliferation, Col-1 and ALP were regarded as biomarkers of early osteogenesis differentiation stage.[33,34] Clo-1 comprises the majority of the extracellular matrix in bone formation.[35] ALP catalyzes the hydrolysis of monoesters of phosphoric acid to generate inorganic phosphate, which is essential for bone mineralization. Elevated levels of Col-1 or ALP can indicate bone healing.[36,37] To assess the role of Lys-AuNCs on MC3T3E-1 osteogenic activities, these two biomarkers were examined using WB and confocal fluorescent imaging. The confocal fluorescent imaging results indicate both Col-1 levels and ALP levels increased when MC3T3E-1 cells were treated with Lys-AuNCs (Figure 2A and B). Meanwhile, the WB results also showed that Col-1 and ALP levels increased, which is in agreement with the imaging study (Figure 2C and D). The higher expression of these two biomarkers provided evidence that the presence of Lys-AuNCs stimulated an early stage of osteoblastic differentiation. Recent studies have demonstrated that AuNPs could promote the Col-1 or ALP activities of MC3T3-E1 cells, thus promoting osteogenic differentiation. In our case, the smaller AuNCs stimulated the activities of Col-1 and ALP with similar mechanisms.[38] However, considering the smaller size of AuNCs compared to traditional AuNPs, they may be an excellent replacement of the traditional AuNPs to promote osteoblastic differentiation.

ALP is a predictor of Bone Mineral Density. There the ALP activity was investigated by both ALP staining and spectrophotometry using MC3T3E-1. High expression of ALP was observed after treatment with Lys-AuNCs by ALP staining (Figure 3A), which was in agreement with the ALP Activity Assay Kit results (Figure 3C). The enhanced ALP activities confirm

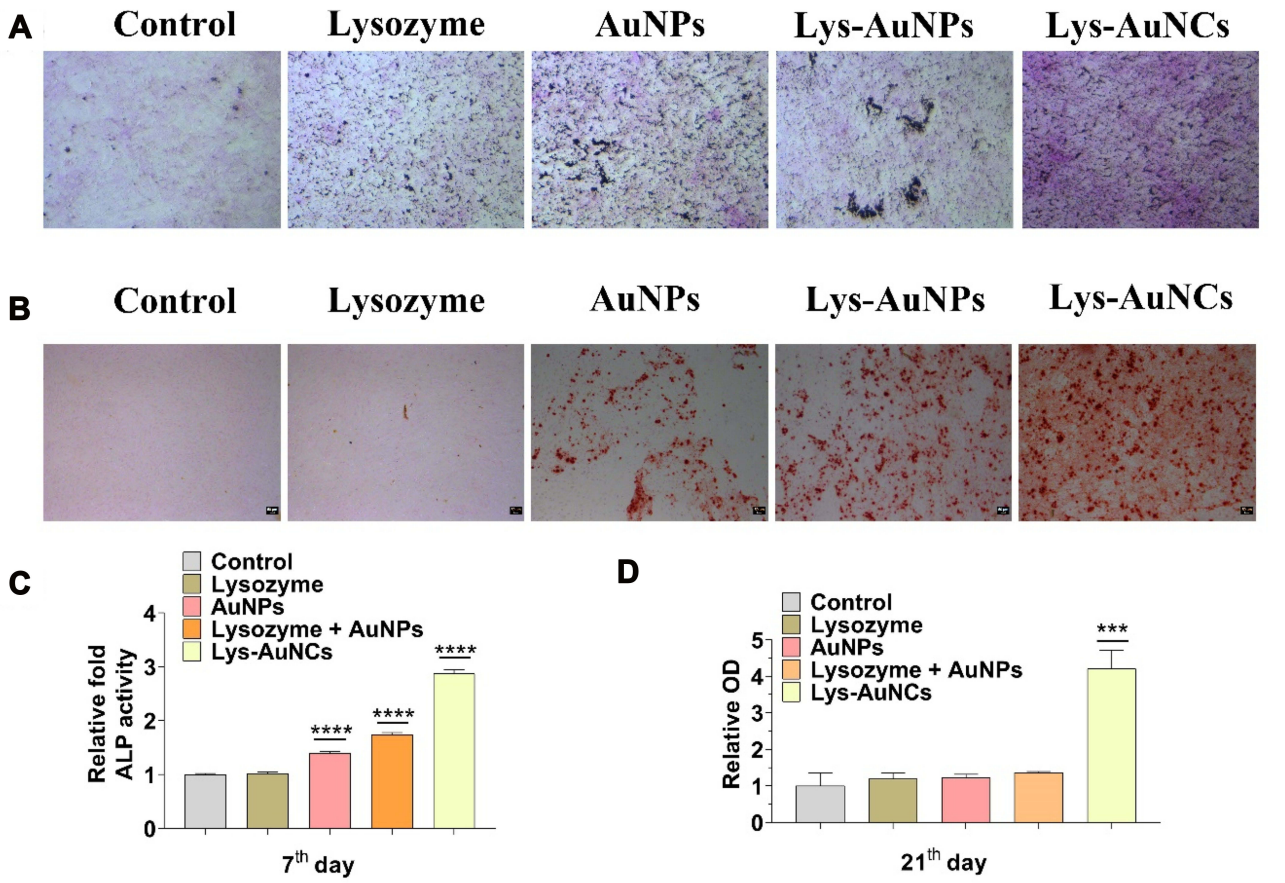

Figure 3 (**A**) ALP stainings of MC3T3E-1 cells (control groups: without any treatment; lysozyme groups: 50 μM lysozyme; lysozyme-AuNCs groups: 50 μM lysozyme-AuNCs). (**B**) Alizarin red staining of MC3T3E-1 cells. (**C**) Relative ALP activity of MC3T3E-1 cells after 7 days of osteogenesis by spectrophotometry at 405 nm. Data from all three experiments are presented as mean ± SD. Scale bar = 100 μm, ****P < 0.001, ***P < 0.001 vs control group.. (**D**) Bar graph of quantitative alizarin red staining by spectrophotometry at 562 nm. Data from all three experiments are presented as mean ± SD.

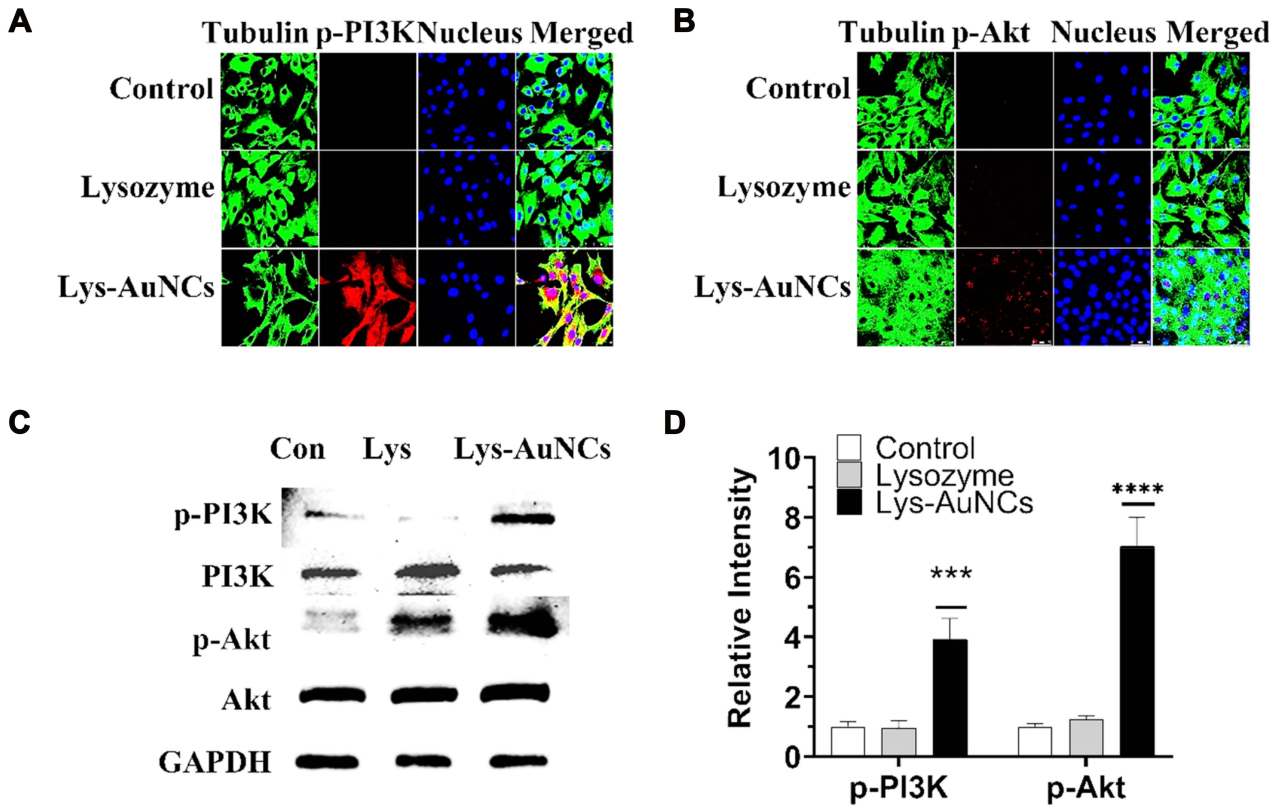

Figure 4 Lys-AuNCs activated the PI3K/Akt signaling pathway. Confocal fluorescence imaging analyses showed that effects of Lys-AuNCs on protein expression of p-PI3K (**A**) and p-Akt (**B**) of MC3T3E-1 cells. (**C**) WB analyses of specific proteins in PI3K/Akt pathways on 3 days of MC3T3E-1 cells. (**D**) Relative quantitative analysis of WB analyses. Data from all five experiments are presented as mean ± SD. *** and **** $P < 0.001$ vs control group.

that Lys-AuNCs promote early osteogenic differentiation. Calcium deposition was used as an indicator of late-stage osteogenesis and maturation of osteoblast differentiation. The calcium deposition was examined by Alizarin Red Staining (ARS) and quantified on the 21st day. Consistent with the results of ARS (Figure 3B), more calcium deposition was also observed in the Lys-AuNCs group measuring by quantitative analysis of alizarin red by UV-vis at 562 nm (Figure 3D). For comparison, the ALP activity and the calcium deposition were also investigated by using lysozyme, AuNPs, a mixture of lysozyme and AuNPs. However, these agents all show insignificant influence on the promotion of these two factors. The higher expressions of the biomarkers including Col-1, ALP, and the enhancement of the calcium deposition by using Lys-AuNCs all indicate Lys-AuNCs remarkably promote the osteogenic activity at both early and late stages.

The PI3K/Akt are important cellular signal transduction pathways, which play vital roles in mediating many processes, including cell proliferation, cell differentiation, apoptosis, and necrosis.[39] To further explore the mechanism for the MC3T3-E1 cell differentiation, typical signaling pathways involved in osteogenesis PI3K/Akt[40] were examined by WB and fluorescent cell imaging (Figure 4). According to the fluorescent cell imaging (Figure 4A and B) and the WB results (Figure 4C and D). It is promising to find that the higher expressions of p-PI3K and p-Akt were both observed in the Lys-AuNCs group.

Inhibition of Osteoclastogenesis

Therapeutic approaches for inhibiting osteoclastogenesis have been proven to be efficient to prevent osteoporosis.[41] TRAP is a histochemical biomarker of osteoclastogenesis.[42–44] The overexpression of TRAP has also been suggested to be involved in the bone resorptive activity of osteoclasts.[45,46] To verify the effects of lysozyme and Lys-AuNCs on inhibiting the negative influence of osteoporosis, a typical macrophage-like cell line (Raw 264.7) was used (Figure 5). Raw 264.7 cells were cultured with 50 μM of different agents in the presence of RANKL for 5 days. It can be seen from Figure 5A (fluorescent cell imaging) that the TRAP expression was significantly

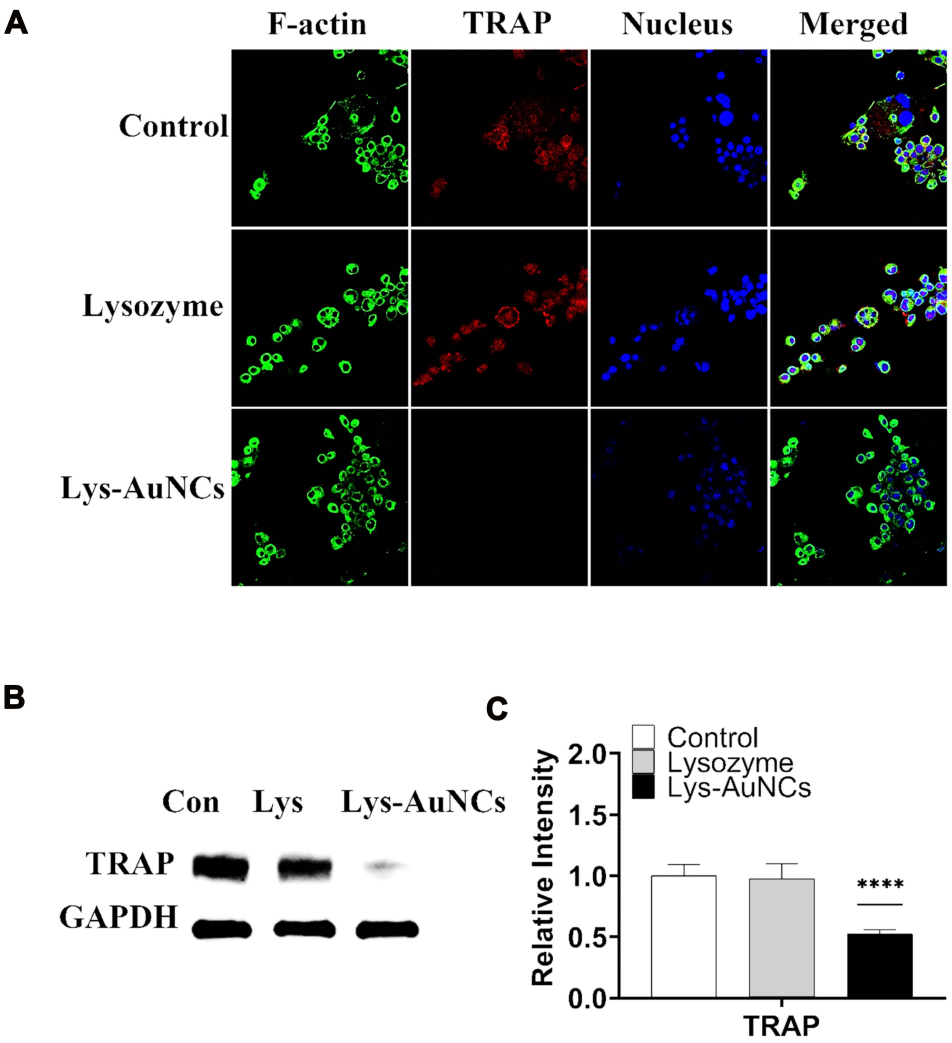

Figure 5 (**A**) Confocal fluorescence imaging analyses showed that the effects of Lys-AuNCs on protein expression of TRAP for RANKL-induced Raw 264.7 cells. (**B**) WB analyses of TRAP after 5 days of RANKL-induced Raw 264.7 cells. (**C**) Relative quantitative analysis of WB analyses. Data from all five experiments are presented as mean ± SD. ****P < 0.001.

suppressed by treatment with Lys-AuNCs. Meanwhile, the WB is in good agreement with this result (Figure 5B and C). This implies that Lys-AuNCs are effective for the inhibition of osteoclastogenesis through the decrease of TRAP.

During osteoclastogenesis, the biomarkers such as c-Fos can enhance NFATc1 expression by RANKL stimulation.[47–50] Meanwhile, V-ATPase-d2, CTSK, and TRAP[51] can also be enhanced. To further investigate the influence of Lys-AuNCs on osteoclastogenesis, these biomarkers are investigated by RANKL-induced Raw 264.7 cells. The fluorescent cell imaging and WB are shown in Figure 6. As shown by the cell imaging results (Figure 6A), the NFATc-1 was attenuated by Lys-AuNCs. In addition, Lys-AuNCs also suppressed the protein expression levels of c-Fos, V-ATPase-d2, and CTSK (Figure 6B and C) based on the WB investigation. The decrease of these biomarkers further confirms that Lys-AuNCs excellently inhibits osteoclastogenesis.

Based on the above studies, the potential of using AuNCs for osteoporosis therapy is summarized (Figure 7). Lys-AuNCs promote the cell proliferation rate of osteoblast. One of the reasons was possibly caused by their antibacterial effect.[52] This antibacterial effect of Lys-AuNCs during the proliferation of osteoblast will be further investigated in the future. Meanwhile, they increased protein expressions such as Col-1 and ALP, which can promote PI3K/Akt signaling pathways. They can also downregulate the protein expression of factors such as

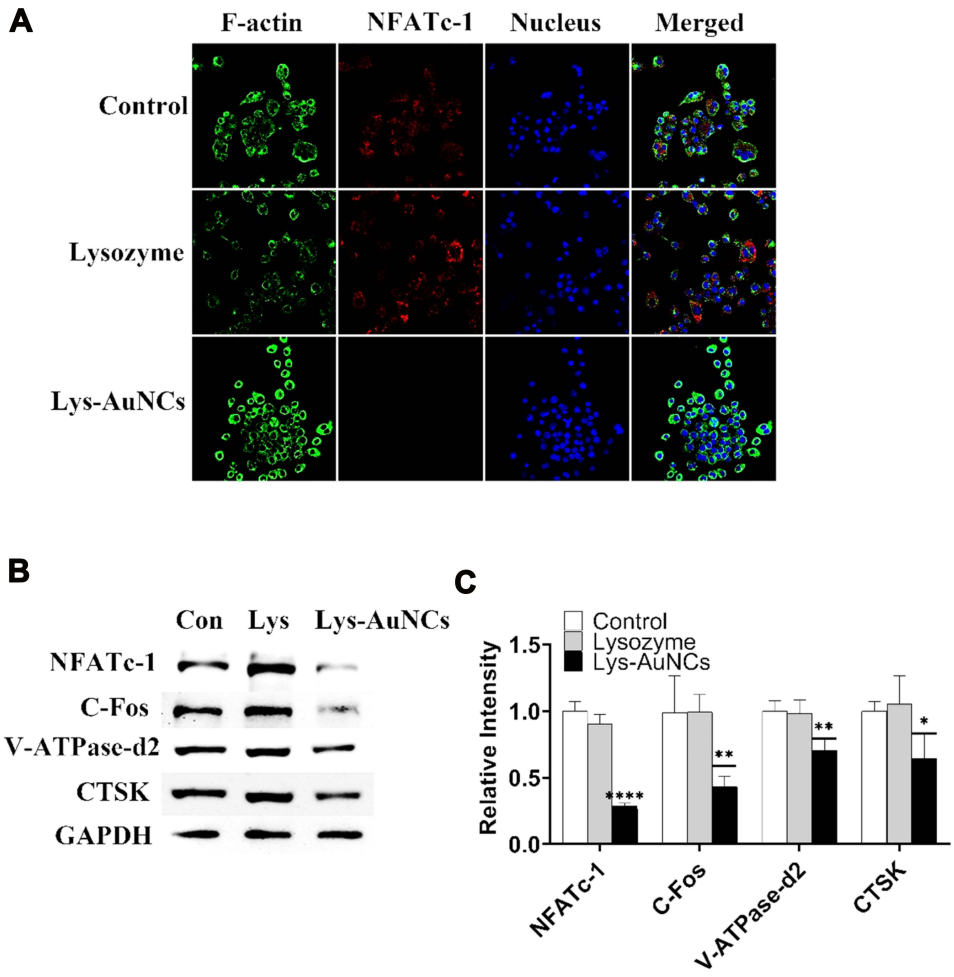

Figure 6 (**A**) Confocal fluorescence imaging of NFATc-1 of TRAP-induced in Raw 264.7 cells cultures. (**B**) WB analyses of specific proteins in NFATc-1/c-Fos/V-ATPase-d2 /CTSK signaling pathway after 5 days of RANKL-induced Raw 264.7 cells. (**C**) Quantification of the ratios of band intensity of NFATc-1, c-Fos, V-ATPase-d2 and CTSK relative to GAPDH. All bar charts are presented as mean ± SD; n=5. *p<0.05, ****p<0.001 relative to non-treatment group, ** indicates $P < 0.01$ vs control group.

TRAP and NFATc-1, which will inhibit NFATc-1/c-Fos/ V-ATPase-d2/CTSK signaling pathways. The development of low-toxic osteoclast-targeting agents is important for the prevention or treatment of bone diseases and for bone regenerative medicine. AuNCs are quite attractive on their own as a promising medicine that finds extensive use in many biomedical applications such as diagnostics, therapeutics, and theranostics.[53] In the process of bone regeneration, Lys-AuNCs promote osteogenic differentiation and inhibit osteoclastogenesis. Accordingly, various other AuNCs might have similar positive effects on the therapy of bone disease. It has been shown by various previous works that AuNCs have no drug-resistance problems for bacterial infected diseases and little toxicity problems are found for the mammalian animals.[54–58] Thus, the development of NCs are very promising for the prevention of osteoporosis and other bone diseases.

Conclusion

In conclusion, Lys-AuNCs can be promising nanomedicines for the therapy of osteoporosis by the promotion of osteogenesis and the inhibition of osteoclastogenesis. Notably, the in vitro study shows that they are associated with the increase of protein expression of Col-1 and ALP, which can promote PI3K/Akt signaling pathways. They can also downregulate of protein expression of TRAP and NFATc-1, which will inhibit NFATc-1/c-Fos//V-ATPase-d2 /CTSK signaling pathways. These results revealed that AuNCs could cure osteoporosis of different aspects. We propose an ultra-small and biocompatible nanomaterial for

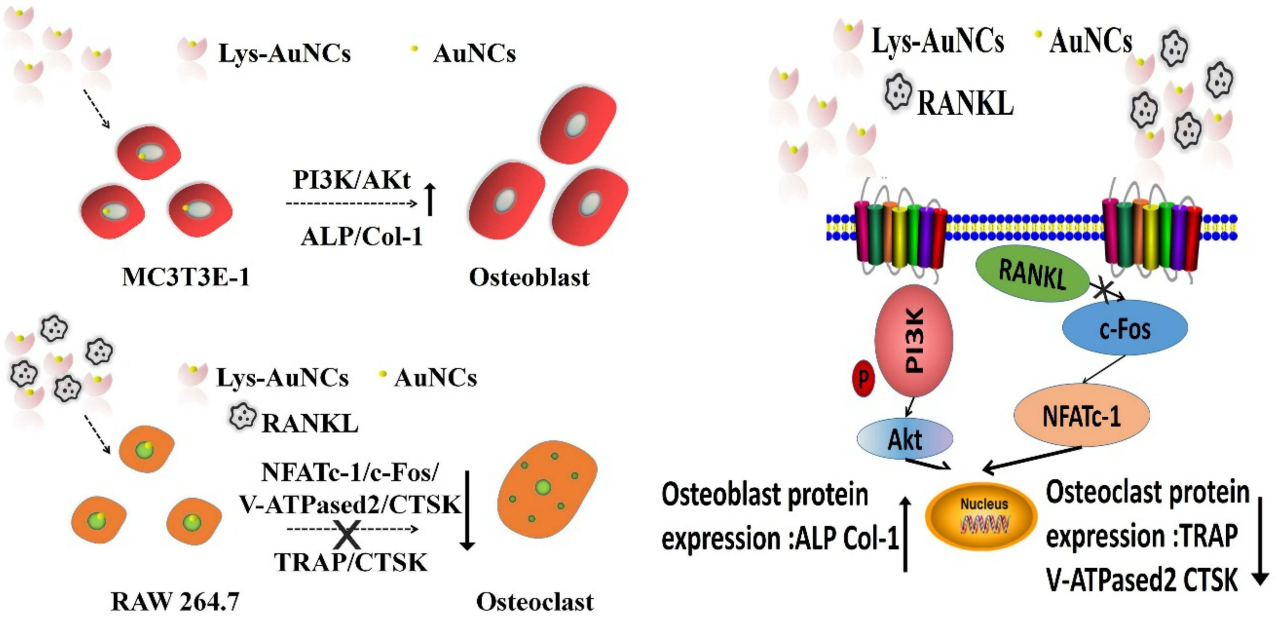

Figure 7 The scheme diagram illustrated that Lys-AuNCs might upregulate the phosphorylated level of PI3K and Akt, and promoted the expression of osteogenic related proteins. Meanwhile, Lys-AuNCs inhibited the osteoclast-related proteins such as TRAP, NFATc-1, c-Fos, V-ATPase-d2 and CTSK.

therapy of osteoporosis, which would be very useful in the development of an in vivo drug in this area.

Acknowledgments

This work was supported by the National Natual Science Foundation of China (NSFC) (NO. 81671907, 81871556).

Disclosure

The authors report no conflicts of interest in this work.

References

1. Lems WF, Raterman HG. Critical issues and current challenges in osteoporosis and fracture prevention. An overview of unmet needs. *Ther Adv Musculoskelet Dis*. 2017;9(12):299–316. doi:10.1177/1759720X17732562
2. Tao B, Zhao W, Lin C, et al. Surface modification of titanium implants by ZIF-8@Levo/LBL coating for inhibition of bacterial-associated infection and enhancement of in vivo osseointegration. *Chem Eng J*. 2020;390:124621.
3. Adami G, Jaleel A, Curtis JR, et al. Temporal trends and factors associated with bisphosphonate discontinuation and restart. *J Bone Mineral Res*. 2019;35:478–487.
4. Reid IR, Bolland MJ. Controversies in medicine: the role of calcium and vitamin D supplements in adults. *Med J Aust*. 2019;211(10):468–473. doi:10.5694/mja2.50393
5. Chen JF, Lin PW, Tsai YR, Yang YC, Kang HY. Androgens and androgen receptor actions on bone health and disease: from androgen deficiency to androgen therapy. *Cells*. 2019;8(11):1318. doi:10.3390/cells8111318
6. Compston JE, McClung MR, Leslie WD. Osteoporosis. *Lancet*. 2019;393(10169):364–376. doi:10.1016/S0140-6736(18)32112-3
7. Khosla S, Hofbauer LC. Osteoporosis treatment: recent developments and ongoing challenges. *Lancet Diabetes Endocrinol*. 2017;5(11):898–907. doi:10.1016/S2213-8587(17)30188-2
8. Fernandes G, Yang S. Application of platelet-rich plasma with stem cells in bone and periodontal tissue engineering. *Bone Res*. 2016;4(1):16036. doi:10.1038/boneres.2016.36
9. Lampe JN, Kim H-J, Jeong HE, Bae J-H, Baek Y-H, Shin J-Y. Characteristics and trends of spontaneous reporting of therapeutic ineffectiveness in South Korea from 2000 to 2016. *PLoS One*. 2019;14(2):e0212905. doi:10.1371/journal.pone.0212905
10. Lloyd AA, Gludovatz B, Riedel C, et al. Atypical fracture with long-term bisphosphonate therapy is associated with altered cortical composition and reduced fracture resistance. *Proc Natl Acad Sci U S A*. 2017;114(33):8722–8727. doi:10.1073/pnas.1704460114
11. Gonc EN, Ozon A, Buyukyilmaz G, Alikasifoglu A, Simsek OP, Kandemir N. Acquired resistance to pamidronate treated effectively with zoledronate in juvenile Paget's disease. *Osteoporosis Int*. 2018;29(6):1471–1474. doi:10.1007/s00198-018-4443-7
12. de Carvalho JO, de Carvalho Oliveira F, Freitas SAP, et al. Carbon nanomaterials for treating osteoporotic vertebral fractures. *Curr Osteoporos Rep*. 2018;16(5):626–634. doi:10.1007/s11914-018-0476-2
13. Cheng H, Chawla A, Yang Y, et al. Development of nanomaterials for bone-targeted drug delivery. *Drug Discov Today*. 2017;22(9):1336–1350. doi:10.1016/j.drudis.2017.04.021
14. Liang H, Xu X, Feng X, et al. Gold nanoparticles-loaded hydroxyapatite composites guide osteogenic differentiation of human mesenchymal stem cells through Wnt/beta-catenin signaling pathway. *Int J Nanomedicine*. 2019;14:6151–6163. doi:10.2147/IJN.S213889
15. Choi SY, Song MS, Ryu PD, Lam AT, Joo SW, Lee SY. Gold nanoparticles promote osteogenic differentiation in human adipose-derived mesenchymal stem cells through the Wnt/beta-catenin signaling pathway. *Int J Nanomedicine*. 2015;10:4383–4392. doi:10.2147/IJN.S78775
16. Niu C, Yuan K, Ma R, et al. Gold nanoparticles promote osteogenic differentiation of human periodontal ligament stem cells via the p38 MAPK signaling pathway. *Mol Med Rep*. 2017;16(4):4879–4886. doi:10.3892/mmr.2017.7170

17. Zeng L, Geng H, Gu W, et al. Au nanoparticles attenuate RANKL-induced osteoclastogenesis by suppressing pre-osteoclast fusion. *J Nanosci Nanotechnol*. 2019;19(4):2166–2173. doi:10.1166/jnn.2019.15764
18. Pan T, Song W, Gao H, et al. miR-29b-loaded gold nanoparticles targeting to the endoplasmic reticulum for synergistic promotion of osteogenic differentiation. *ACS Appl Mater Interfaces*. 2016;8(30):19217–19227. doi:10.1021/acsami.6b02969
19. Lomeli-Marroquin D, Medina Cruz D, Nieto-Arguello A, et al. Starch-mediated synthesis of mono- and bimetallic silver/gold nanoparticles as antimicrobial and anticancer agents. *Int J Nanomedicine*. 2019;14:2171–2190. doi:10.2147/IJN.S192757
20. Bolanos K, Kogan MJ, Araya E. Capping gold nanoparticles with albumin to improve their biomedical properties. *Int J Nanomedicine*. 2019;14:6387–6406. doi:10.2147/IJN.S210992
21. Zheng Y, Lai L, Liu W, Jiang H, Wang X. Recent advances in biomedical applications of fluorescent gold nanoclusters. *Adv Colloid Interface Sci*. 2017;242:1–16. doi:10.1016/j.cis.2017.02.005
22. Kaur N, Aditya RN, Singh A, Kuo TR. Biomedical applications for gold nanoclusters: recent developments and future perspectives. *Nanoscale Res Lett*. 2018;13(1):302. doi:10.1186/s11671-018-2725-9
23. De Matteis V, Malvindi MA, Galeone A, et al. Negligible particle-specific toxicity mechanism of silver nanoparticles: the role of Ag+ ion release in the cytosol. *Nanomedicine*. 2015;11(3):731–739. doi:10.1016/j.nano.2014.11.002
24. Zhang P, Li D, Chen G, Mei X, Zhang J, Chen Z. Preparation of tea polyphenol-modified copper nanoclusters to promote the proliferation of MC3T3-E1 in high glucose microenvironment. *N J Chem*. 2019;43(10):4082–4091. doi:10.1039/C8NJ06002A
25. Shi YE, Luo S, Ji X, et al. Synthesis of ultra - stable copper nanoclusters and their potential application as a reversible thermometer. *Dalton Trans*. 2017;46(41):14251–14255. doi:10.1039/C7DT02193C
26. Jin R. Atomically precise metal nanoclusters: stable sizes and optical properties. *Nanoscale*. 2015;7(5):1549–1565. doi:10.1039/C4NR05794E
27. Zhang Q, Yang M, Zhu Y, Mao C. Metallic nanoclusters for cancer imaging and therapy. *Curr Med Chem*. 2018;25(12):1379–1396. doi:10.2174/0929867324666170331122757
28. Li D, Kumari B, Makabenta JM, Gupta A, Rotello V. Effective detection of bacteria using metal nanoclusters. *Nanoscale*. 2019;11(46):22172–22181. doi:10.1039/C9NR08510F
29. Gao G, Chen R, He M, et al. Gold nanoclusters for Parkinson's disease treatment. *Biomaterials*. 2019;194:36–46. doi:10.1016/j.biomaterials.2018.12.013
30. Zhang XD, Luo Z, Chen J, et al. Ultrasmall glutathione-protected gold nanoclusters as next generation radiotherapy sensitizers with high tumor uptake and high renal clearance. *Sci Rep*. 2015;5(1):8669. doi:10.1038/srep08669
31. Zhao L, Jiang D, Cai Y, Ji X, Xie R, Yang W. Tuning the size of gold nanoparticles in the citrate reduction by chloride ions. *Nanoscale*. 2012;4(16):5071–5076. doi:10.1039/c2nr30957b
32. Li D, Zhuang P, Li K, Qian K, Mei X. Fabrication of antibacterial sponge cleaner using gold nanoclusters. *IET Nanobiotechnol*. 2020.
33. Mao S-H, Chen C-H, Chen C-T. Osteogenic potential of induced pluripotent stem cells from human adipose-derived stem cells. *Stem Cell Res Ther*. 2019;10(1). doi:10.1186/s13287-019-1402-y
34. Molagoda IMN, Karunarathne WAHM, Choi YH, et al. Fermented oyster extract promotes osteoblast differentiation by activating the Wnt/β-catenin signaling pathway, leading to bone formation. *Biomolecules*. 2019;9(11):711. doi:10.3390/biom9110711
35. Zhao M, Altankov G, Grabiec U, et al. Molecular composition of GAG-collagen I multilayers affects remodeling of terminal layers and osteogenic differentiation of adipose-derived stem cells. *Acta Biomater*. 2016;41:86–99. doi:10.1016/j.actbio.2016.05.023
36. Millan JL. Alkaline Phosphatases: structure, substrate specificity and functional relatedness to other members of a large superfamily of enzymes. *Purinergic Signal*. 2006;2(2):335–341. doi:10.1007/s11302-005-5435-6
37. Zhang K, Jia Z, Yang B, et al. Adaptable hydrogels mediate cofactor-assisted activation of biomarker-responsive drug delivery via positive feedback for enhanced tissue regeneration. *Adv Sci*. 2018;5(12):1800875. doi:10.1002/advs.201800875
38. Li J, Li JJ, Zhang J, Wang X, Kawazoe N, Chen G. Gold nanoparticle size and shape influence on osteogenesis of mesenchymal stem cells. *Nanoscale*. 2016;8(15):7992–8007. doi:10.1039/C5NR08808A
39. Yu JS, Cui W. Proliferation, survival and metabolism: the role of PI3K/AKT/mTOR signalling in pluripotency and cell fate determination. *Development*. 2016;143(17):3050–3060. doi:10.1242/dev.137075
40. Liu MZ, Zhou DC, Liu Q, et al. Osteogenesis activity of isocoumarin a through the activation of the PI3K-Akt/Erk cascade-activated BMP/RUNX2 signaling pathway. *Eur J Pharmacol*. 2019;858:172480. doi:10.1016/j.ejphar.2019.172480
41. Liu Y, Wang C, Wang G, et al. Loureirin B suppresses RANKL-induced osteoclastogenesis and ovariectomized osteoporosis via attenuating NFATc1 and ROS activities. *Theranostics*. 2019;9(16):4648–4662. doi:10.7150/thno.35414
42. Behrends DA, Hui D, Gao C, et al. Defective bone repair in C57Bl6 mice with acute systemic inflammation. *Clin Orthop Relat Res*. 2017;475(3):906–916. doi:10.1007/s11999-016-5159-7
43. Egusa H, Kaneda Y, Akashi Y, et al. Enhanced bone regeneration via multimodal actions of synthetic peptide SVVYGLR on osteoprogenitors and osteoclasts. *Biomaterials*. 2009;30(27):4676–4686. doi:10.1016/j.biomaterials.2009.05.032
44. Briggs TA, Rice GI, Adib N, et al. Spondyloenchondrodysplasia due to mutations in ACP5: a comprehensive survey. *J Clin Immunol*. 2016;36(3):220–234. doi:10.1007/s10875-016-0252-y
45. Angel NZ, Walsh N, Forwood MR, Ostrowski MC, Cassady AI, Hume DA. Transgenic mice overexpressing tartrate-resistant acid phosphatase exhibit an increased rate of bone turnover. *J Bone Mineral Res*. 2000;15(1):103–110. doi:10.1359/jbmr.2000.15.1.103
46. Suh KS, Chon S, Jung WW, Choi EM. Effects of methylglyoxal on RANKL-induced osteoclast differentiation in Raw 264.7cells. *Chem Biol Interact*. 2018;296:18–25. doi:10.1016/j.cbi.2018.09.005
47. Asagiri M, Sato K, Usami T, et al. Autoamplification of NFATc1 expression determines its essential role in bone homeostasis. *J Exp Med*. 2005;202(9):1261–1269. doi:10.1084/jem.20051150
48. Pan MG, Xiong Y, Chen F. NFAT gene family in inflammation and cancer. *Curr Mol Med*. 2013;13(4):543–554. doi:10.2174/1566524011313040007
49. Takayanagi H, Kim S, Koga T, et al. Induction and activation of the transcription factor NFATc1 (NFAT2) integrate RANKL signaling in terminal differentiation of osteoclasts. *Dev Cell*. 2002;3(6):889–901. doi:10.1016/S1534-5807(02)00369-6
50. Xiao Y, Li K, Wang Z, et al. Pectolinarigenin prevents bone loss in ovariectomized mice and inhibits RANKL-induced osteoclastogenesis via blocking activation of MAPK and NFATc1 signaling. *J Cell Physiol*. 2019;234(8):13959–13968. doi:10.1002/jcp.28079
51. Chen X, Chen X, Zhou Z, et al. LY411575, a potent gamma-secretase inhibitor, suppresses osteoclastogenesis in vitro and LPS-induced calvarial osteolysis in vivo. *J Cell Physiol*. 2019;234(11):20944–20956. doi:10.1002/jcp.28699
52. Kalita S, Kandimalla R, Bhowal AC, Kotoky J, Kundu S. Functionalization of beta-lactam antibiotic on lysozyme capped gold nanoclusters retrogress MRSA and its persisters following awakening. *Sci Rep*. 2018;8(1):5778. doi:10.1038/s41598-018-22736-5

53. Li L, Zhang L, Wang T, et al. Facile and scalable synthesis of novel spherical au nanocluster assemblies@polyacrylic acid/calcium phosphate nanoparticles for dual-modal imaging-guided cancer chemotherapy. *Small*. 2015;11(26):3162–3173. doi:10.1002/smll.201403517
54. Yougbare S, Chang TK, Tan SH, et al. Antimicrobial gold nanoclusters: recent developments and future perspectives. *Int J Mol Sci*. 2019;20(12):2924. doi:10.3390/ijms20122924
55. Li Y, Zhen J, Tian Q, et al. One step synthesis of positively charged gold nanoclusters as effective antimicrobial nanoagents against multidrug-resistant bacteria and biofilms. *J Colloid Interface Sci*. 2020;569:235–243. doi:10.1016/j.jcis.2020.02.084
56. Loynachan CN, Soleimany AP, Dudani JS, et al. Renal clearable catalytic gold nanoclusters for in vivo disease monitoring. *Nat Nanotechnol*. 2019;14(9):883–890. doi:10.1038/s41565-019-0527-6
57. Xie Y, Liu Y, Yang J, et al. Gold nanoclusters for targeting methicillin-resistant staphylococcus aureus in vivo. *Angew Chem Int Ed Engl*. 2018;57(15):3958–3962. doi:10.1002/anie.201712878
58. Wang L, Zheng W, Jiang X. Benzeneselenol-modified gold nanoclusters for cancer therapy. *Chem Commun*. 2020.